Polyhedron 73 (2014) 51–58

Contents lists available at ScienceDirect

Polyhedron

journal homepage: www.elsevier.com/locate/poly

Crystal structure, vibrational and thermal behavior of $Ba(NH_4)[Co(CN)_6]\cdot 4H_2O$: A new precursor for the synthesis of hexagonal $BaCoO_3$

Diego M. Gil [a], Alejandro Di Santo [a], Fernando Pomiro [c], Gustavo A. Echeverría [b,1], Oscar E. Piro [b,1], Raúl E. Carbonio [c,*,1], Aida Ben Altabef [a,*,1]

[a] INQUINOA, CONICET, Instituto de Química Física, Facultad de Bioquímica, Química y Farmacia, Universidad Nacional de Tucumán, San Lorenzo 456, T4000CAN San Miguel de Tucumán, Argentina
[b] Departamento de Física, Facultad de Ciencias Exactas, Universidad Nacional de La Plata and Institute IFLP (CONICET, CCT-La Plata), C. C. 67, 1900 La Plata, Argentina
[c] INFIQC (CONICET-Universidad Nacional de Córdoba), Departamento de Fisicoquímica, Facultad de Ciencias Químicas, Universidad Nacional de Córdoba, Ciudad Universitaria, X5000HUA Córdoba, Argentina

ARTICLE INFO

Article history:
Received 19 December 2013
Accepted 11 February 2014
Available online 19 February 2014

Keywords:
Barium and ammonium hexacyanocobaltate(III) tetrahydrate
Structural single-crystal X-ray diffraction
IR and Raman spectroscopy
Powder X-ray diffraction
Thermal decomposition

ABSTRACT

The crystal structure of $Ba(NH_4)[Co(CN)_6]\cdot 4H_2O$ complex was determined by X-ray diffraction methods. It crystallizes in the hexagonal $P6_3/m$ space group with $a = b = 7.6882(2)$ Å, $c = 14.4764(4)$ Å, and $Z = 2$ molecules per unit cell. The structure was solved from 475 reflections with $I > 2\sigma(I)$ and refined to an agreement R1-factor of 0.0214. The cobaltocyanide anion has an octahedral shape with its Co(III) ion sited at a crystallographic special position of point symmetry $\bar{3}$ (S_6) [d(Co-C) = 1.886(3) Å and d(C–N) = 1.143(4) Å]. The barium ion is in a 9-fold environment at a crystal special position $\bar{6}$ (C_{3h}), coordinated to cyanide N-atoms of neighboring complexes [d(Ba–N) = 2.862(3) Å] and to one type of water molecule laying onto an m mirror plane [d(Ba–Ow) = 2.924(4) Å]. The ammonium ion and the other type of water molecule share four symmetry-related C_3 lattice sites with equal occupancy. Under the $P6_3$ subspace group these four sites split into two independent pairs of C_3 sites, one occupied by two symmetry-related ammonium ions, the other by two (disordered) water molecules. The complex was characterized by UV–Vis, IR and Raman spectroscopy and the thermal decomposition was studied to investigate the formation of $BaCoO_{3-\delta}$. This compound, in its hexagonal form, could be synthesized at temperatures as low as 675 °C. At 750 °C a new orthorhombic poly-type is obtained in a mixture with the hexagonal form which is associated with the appearance of oxygen vacancies. These temperatures of synthesis and reaction times are lower than those reported by ceramic and sol–gel synthesis. These soft treatments gave rise to homogeneous particles of small grain size.

1. Introduction

The structure and properties of different hexacyanometallates(III) hydrates, namely $A[M(CN)_6]\cdot nH_2O$ (A = transition metals, lanthanide; M = transition metals), have been widely investigated for a long time [1–5]. Generally, in hexacyanometallates the metal centers are usually found bridged by CN groups where the C and N ends remain linked to only one metal. The transition metal bonded to the C end is present in octahedral coordination to form the anionic hexacyanometallate octahedral block, $[M^n(CN)_6]^{6-n}$. The 3D framework is formed when neighboring blocks are linked at their N end through a second metal (transition metal, lanthanide or alkaline earth metals). Transition metal cyanides form a particular class of molecular materials where the metal centers remain strongly linked through CN groups, a fact that allows considerable spin coupling and, as a consequence, magnetic order in many of them. Owing to this characteristic these compounds have been extensively studied as prototype of high temperature molecular magnets [1–5].

It is well-known that perovskite-type oxides could be used as catalyst in different chemical reactions, such as oxidation of hydrocarbons [6], for chlorinated volatile organic compounds [7] and decomposition of NO [8]. However, the catalysis with perovskite-type oxides is considered to be far from practical use because of extremely small specific surface area. Therefore, various methods of synthesis have been used for the synthesis of perovskite-type

* Corresponding authors. Tel.: +54 381 4311044; fax: +54 381 4248169 (A. Ben Altabef).
E-mail addresses: carbonio@mail.fcq.unc.edu.ar (R.E. Carbonio), altabef@fbqf.unt.edu.ar (A. Ben Altabef).
[1] Members of the Research Career of CONICET.

http://dx.doi.org/10.1016/j.poly.2014.02.014
0277-5387/

oxides with high specific surface area, including sol–gel synthesis [9–12], co-precipitation [10,12,13], citrate route [9,12], reverse micelle [14] and polymeric precursor methods [15,16]. These methods are primarily intended to prepare the mixed oxides with perovskite structure at temperatures as low as possible for obtaining high specific surface area materials. However, the preparation at low calcination temperatures gives rise to new problems such as poor degree of crystallinity and low homogeneity of chemical composition in desired perovskite-type oxide. The thermal decomposition of hetero-nuclear cyano complexes was proposed by Gallagher in 1968 to prepare $LaFeO_3$ and $LaCoO_3$ from hexacyanometallates as precursors [17]. The oxides obtained by this method were formed at shorter annealing times and lower temperatures than by ceramic methods. The use of a precursor containing the appropriate A/B ratio enforces the formation of ABO_3 perovskite-type oxides with the precise stoichiometry, thus controlling and preventing any elements segregation generally observed in conventional methods and allowing the synthesis of the desired mixed oxide at very low temperatures [18–21].

We report here the synthesis, crystal structure and vibrational characterization of $Ba(NH_4)[Co(CN)_6]\cdot 4H_2O$ and its thermal decomposition products. The crystal structure of the complex was solved by single-crystal X-ray diffraction methods. These measurements were complemented by thermo-gravimetric and differential thermal analysis (TGA-DTA) and UV–visible, IR and Raman spectroscopy and the crystal structure refinements of obtained $BaCoO_{3-\delta}$ was performed by Rietveld analysis of powder X-ray diffraction data (PXRD).

2. Experimental

2.1. Synthesis

The synthesis of $Ba(NH_4)[Co(CN)_6]\cdot 4H_2O$ was performed in two steps [21]. The first one corresponds to the preparation of $Ag_3[Co(CN)_6]$, which was obtained by mixing aqueous solutions of $K_3[Co(CN)_6]$ and $AgNO_3$ in stoichiometric quantities under continuous stirring during 30 min. The white precipitate was separated by filtration and stored in a dry box with $CaCl_2$. In the second step, a mixture of NH_4Cl and $BaCl_2$ was added to a suspension of $Ag_3[Co(CN)_6]$ in water, maintaining the mixture under vigorous stirring during 2 h. The AgCl formed was filtered out and the solution containing $Ba(NH_4)[Co(CN)_6]$ was concentrated at room temperature. Adequate single crystals for structural X-ray diffraction work were obtained from slow evaporation at 20 °C of concentrated aqueous solutions of $Ba(NH_4)[Co(CN)_6]$.

The solid state properties of the obtained material were studied with single-crystal and powder X-ray diffraction methods, UV–Vis, infrared and Raman spectroscopies and thermogravimetric and differential thermal analysis (TGA-DTA).

2.2. Characterization

2.2.1. Crystallographic data and structure determination

The measurements were performed on an Oxford Xcalibur Gemini, Eos CCD diffractometer with graphite-monochromated Co Kα (λ = 0.71073 Å) radiation. X-ray diffraction intensities were collected (ω scans with ϑ and κ-offsets), integrated and scaled with CrysAlisPro [22] suite of programs. The unit cell parameters were obtained by least-squares refinement (based on the angular settings for all collected reflections with intensities larger than seven times the standard deviation of measurement errors) using CrysAlisPro. Data were corrected for extinction and (empirically) for absorption employing the multi-scan method implemented in CrysAlisPro.

From the observed Laue symmetry and extinctions there were two possible space groups, namely the centrosymmetric $P6_3/m$ and its subgroup $P6_3$. As the intensities statistics pointed to the non-centrosymmetric space group, the structure was solved in $P6_3$ by direct methods with SHELXS-97 [23] and the molecular model developed by alternated cycles of Fourier methods and full-matrix least-squares refinement on F^2 with SHELXL-97 [24]. The refinement, though achieving reasonable good agreement R1-factor, showed several anomalies including strong correlation between the atomic parameters of the two independent (in $P6_3$) cyanide groups and the ones of the ammonium N-atom and the oxygen of one type of crystallization water molecule. At this point a test on missed symmetry with the MISSYM (ADDSYM) algorithm [25] showed that the constellation of non-H atoms was in fact centrosymmetric. Interestingly, this higher symmetry is only very weakly disrupted by the difference between the isoelectronic ammonium and water molecules mentioned above. We therefore proceeded to refine the structure in the $P6_3/m$ space group which renders these molecules to be equivalent to each other. They were refined with equal occupancy factors and anisotropic displacement parameters for the nitrogen and oxygen atoms. A Fourier difference map phased on the heavier atoms showed one of the two non-equivalent ammonium H-atoms. This was refined with a isotropic displacement parameter and the N–H and H···H distances respectively constrained to target values of 0.86(1) and 1.39(2) Å to impose tetrahedral N–H bonding. The other ammonium and the water H-atoms could not be reliably located and therefore they were not included in the final molecular model. Crystal data and structure refinement results are summarized in Table 1.

2.2.2. Physical measurements

The UV–Vis spectra of the complex in aqueous solutions were recorded on a Beckman DU 7500 spectrophotometer in the range from 200 to 600 nm.

The infrared spectra of $Ba(NH_4)[Co(CN)_6]\cdot 4H_2O$ at room and low temperatures were recorded in KBr pellets within the 4000–400 cm^{-1} range using a Perkin Elmer GX1 FTIR instrument. A variable temperature RIIC (VLT-2) cell was used to run the spectrum at low temperature (−100 °C) of the complex cooled with air liquid. The Raman spectrum of the solid at room temperature (RT) was measured in the spectral interval from 3500 to 50 cm^{-1} with a Thermoscientific DXR Raman microscope. The Raman data were collected using a diode-pump, solid state laser of 532 nm (at 5 cm^{-1} spectral resolution), a con-focal aperture of 25 μm pinhole, and a 10× objective. The sample was placed on gold-coated sample slides. To achieve a sufficient signal to noise ratio, 30 expositions of 2 s each were accumulated during the measurements with the laser power maintained at 10 mW. The IR and Raman spectra of the thermal decomposition products of $Ba(NH_4)[Co(CN)_6]\cdot 4H_2O$ were measured in the same conditions as for the complex.

Thermogravimetric (TGA) and differential thermal analysis (DTA) measurements were performed with a Shimadzu DTG-60 thermo-balance in the temperature range from 25 to 1000 °C at a heating rate of 5°/min under air flow (90 mL/min).

PXRD patterns were obtained at RT in a PANalytical X'Pert Pro diffractometer (40 kV, 40 mA) in Bragg–Brentano geometry with Cu Kα radiation (λ = 1.5418 Å), between 5° and 120° in 2θ, in steps of 0.02°. The structure refinement using PXRD data were performed by means of the Rietveld method [26] using the Fullprof program [27]. A pseudo-Voigt shape function was found adequate to obtain good fits to experimental data. The following parameters were refined: zero-point, scale factor, background coefficients, pseudo-Voigt parameters for the peak shapes corrected for asymmetry parameters, overall isotropic thermal factor, cell parameters and atomic positions.

Table 1
Crystal data and structure refinement results for $Ba(NH_4)[Co(CN)_6]\cdot 4H_2O$.

Empirical formula	$C_6H_{12}BaCoN_7O_4$
Formula weight	442.50
T (K)	297(2)
Wavelength (Å)	0.71073
Crystal system	hexagonal
Space group	$P6_3/m$
Unit cell dimensions	
a (Å)	7.6882(2)
b (Å)	7.6882(2)
c (Å)	14.4764(4)
γ (°)	120
V (Å^3)	741.04(3)
Z	2
D_{calc} (Mg/m^3)	1.983
Absorption coefficient (mm^{-1})	3.779
$F(000)$	424
Crystal size (mm)	0.287 × 0.262 × 0.081
θ-Range for data collection (°)	3.06–26.99
Index ranges	$-9 \leqslant h \leqslant 6$, $-9 \leqslant k \leqslant 7$, $-18 \leqslant l \leqslant 9$
Reflections collected	1628
Independent reflections (R_{int})	558 (0.0328)
Observed reflections	475
Completeness to θ = 25.98° (%)	99.6
Refinement method	full-matrix least-squares on F^2
Data/restraints/parameters	558/4/37
Goodness-of-fit (GOF) on F^2	1.165
Final R indices [$I > 2\sigma(I)$][a]	R_1 = 0.0214, wR_2 = 0.0524
R indices (all data)	R_1 = 0.0264, wR_2 = 0.0560
Extinction coefficient	0.038(2)
Largest difference in peak and hole (e Å^{-3})	0.438 and −0.389

[a] $R_1 = \sum||F_o| - |F_c||/\sum|F_o|$, $wR_2 = [\sum w(|F_o|^2 - |F_c|^2)^2/\sum w(|F_o|^2)^2]^{1/2}$.

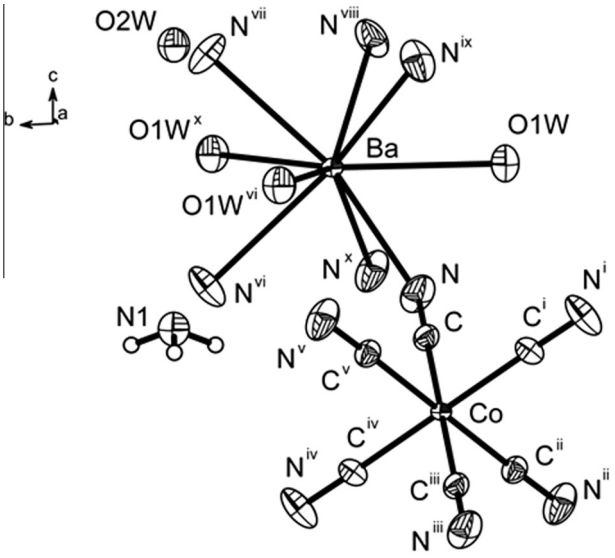

Fig. 1. Plot of $Ba(NH_4)[Co(CN)_6].4H_2O$ showing the labeling of the non-H atoms and their displacement ellipsoids at the 30% probability level. In $P6_3/m$ space group, cobalt is at a site of point symmetry $\bar{3}$, barium at $\bar{6}$, ammonium and one type of (disordered) water molecule (O2w) are at C_3 sites, and the other type of water molecule (O1w) lies onto a mirror m plane. Superscripts indicate equivalent atoms related through the crystal symmetry operations: (i) $-x+y, -x, z$ (ii) $y, -x+y, -z$; (iii) $-x, -y, -z$; (iv) $x-y, x, -z$; (v) $-y, x-y, z$; (vi) $-x+y+1, -x+1, z$; (vii) $-x+y+1, -x+1, -z+1/2$; (viii) $-y+1, x-y, -z+1/2$; (ix) $x, y, -z+1/2$; (x) $-y+1, x-y, z$.

3. Results and discussion

3.1. Crystal structure of $Ba(NH_4)[Co(CN)_6]\cdot 4H_2O$

Fig. 1 shows an ORTEP [28] plot of $Ba(NH_4)[Co(CN)_6]\cdot 4H_2O$ indicating the coordination environment of the metal centers in the complex. Bond distances and angles around cobalt and barium ions are given in Table 2. The hexacyanocobaltate $[Co(CN)_6]^{3-}$ complex has an almost perfect octahedral shape with its Co(III) ion sited at a crystallographic special position of point symmetry $\bar{3}$ (S_6) [d(Co–C) = 1.889(3) Å, d(C–N) = 1.142(4) Å and ∠(Co–N–C) = 178.8(3)°] with *cis* C–Co–C angle equal to 91.3(1)°.

The barium Ba^{2+} ion is in a 9-fold environment at a crystal special position $\bar{6}$ (C_{3h}), coordinated to cyanide N-atoms of neighboring complexes [d(Ba–N) = 2.859(3) Å] and to one type of water molecule [d(Ba-O1w) = 2.923(4) Å]. This water molecule lies onto a m mirror plane. The coordination around Ba^{2+} can be described as a distorted and capped Archimedean anti-prism of nearly rectangular basis rotated from each other in about 45° (see Fig. 1). The alkaline-earth metal is sandwiched between one of the basis with cyanide N-atoms at its four vertices and the other (distorted) rectangular basis conformed by pairs of opposite cyanide nitrogen and water (O1w) oxygen atoms. The 9-fold coordination is completed with a water molecule (O1w) at a capping site above the N_4 rectangular basis. Both metal centers are linked through a cyano bridge. The crystal structure of the studied complex can be considered as the assembly of CoC_6 octahedra and BaN_6O_3 polyhedra to form an infinite polymeric array as shown in Fig. 2. It can also been regarded as $Co(CN)_6$ octahedral blocks bridged by Ba atoms bonded at their N ends. According to the bond angles (Table 2) during the barium salt formation the building unit, $[Co(CN)_6]^{3-}$, approximately preserves its original geometry, however the N–Ba–N bonds deviates from the linearity with an average angle of about 136.6 and 73.3°.

In $P6_3/m$ space group, the ammonium NH_4^+ ion and the water molecule O2w (disordered) share with equal occupancy four symmetry-related C_3 lattice sites, namely (1/3, 2/3, z), (2/3, 1/3, z + 1/2), (2/3, 1/3, $-z$), and (1/3, 2/3, $-z$ + 1/2). The second pair of symmetry operations is related to the first pair through an inversion centre. In the subgroup of lower symmetry $P6_3$ these four sites still retain the C_3 symmetry, but now they are only equivalent within the pairs as the inversion symmetry no longer connect the two pairs. Hence ammonium ion occupy the two symmetry-related (under $P6_3$) sites of one pair, namely (1/3, 2/3, z) and (2/3, 1/3, z + 1/2) and the water molecule O2w the two equivalent sites of the other pair, i.e. (2/3, 1/3, $-z$) and (1/3, 2/3, $-z$ + 1/2).

3.2. UV–Vis spectra of aqueous solutions of $Ba(NH_4)[Co(CN)_6]\cdot 4H_2O$

The UV–Vis absorption spectra of aqueous solutions of $Ba(NH_4)[Co(CN)_6]\cdot 4H_2O$ are compared with $K_3[Co(CN)_6]$ (aq) in Fig. 3 where it can be appreciated the presence of free $[Co(CN)_6]^{3-}$ ions in solution. The features at 259 and 313 nm in the spectrum of aqueous solutions of $Ba(NH_4)[Co(CN)_6]$ appear at similar wavelengths as in the spectrum of aqueous $K_3[Co(CN)_6]$. The two absorption bands observed in the spectra correspond to $^1T_{2g}$, $^1T_{1g} \leftarrow {}^1A_{1g}$ transitions, respectively [29].

3.3. Infrared and Raman spectra

The infrared absorption spectra of $Ba(NH_4)[Co(CN)_6]\cdot 4H_2O$ recorded at room and low temperatures are shown in Fig. 4. The main features of the spectra can be immediately assigned to the internal vibrations of the hexacyanocobaltate(III) anion, the ammonium ion and the water molecules, as well as to the librations of these molecules. The Raman dispersion spectrum of the complex in the solid state at RT is shown in Fig. 5. Wavenumbers of the IR and Raman internal bands of the complex and their tentative assignments are included in Table 3. The assignment of bands were performed by

Table 2
Selected bond lengths (Å) and angles (°) around the metal centers in $Ba(NH_4)[Co(CN)_6]\cdot 4H_2O$.

Bond distances		Bond angles	
Co–C	1.886(3)	C–Co–C^{i}	91.3(1)
Ba–N	2.862(3)	N–Ba–N^{vi}	79.5(1)
Ba–O(1)w	2.924(4)	N–Ba–N^{viii}	136.66(6)
		N–Ba–N^{ix}	84.8(2)
		N–Ba–O(1 W)	68.81(8)
		N–Ba–O(1 W)^{vi}	67.85(9)
		N–Ba–O(1 W)^{x}	137.6(8)

Symmetry transformations used to generate equivalent atoms: (i) $-x+y, -x, z$; (vi) $-x+y+1, -x+1, z$; (viii) $-y+1, x-y, -z+1/2$; (ix) $x, y, -z+1/2$; (x) $-y+1, x-y, z$.

comparison with similar compounds containing the $[Co(CN)_6]^{3-}$ anion [20,30,31].

3.3.1. CN stretching bands

The two strong bands located at 2153 and 2141 cm^{-1} in the Raman spectrum are assigned to the symmetric stretching vibration of the Ba–N≡C–Co bridges. The strong band observed at 2131 cm^{-1} in the IR spectrum at RT (2132 cm^{-1} at LT) is assigned the anti-symmetric stretching mode of the CN bridges. The weak bands observed in the room and low temperatures IR spectra at 2091 cm^{-1} can be assigned to the anti-symmetric stretching mode of the isolated (diluted) isotopic $^{13}C^{14}N$ species due to the presence of ^{13}C in relative natural abundance. It is assumed that the bands due to the $^{13}C^{15}N$ species are too weak to be observed in the IR and Raman spectra. These results are in agreement with the assignment reported for different hexacyanocobaltates(III) [20,30,31].

3.3.2. M–C≡N and M–C bands

The weak band at 565 and 568 cm^{-1} in the RT and LT spectra, respectively, are assigned to Co–C stretching mode of the CoC_6 octahedral core and the band observed at 409 cm^{-1} is assigned to the same mode. The band with medium intensity at 419 cm^{-1} in the IR spectrum at RT (417 cm^{-1} in the Raman spectrum) is assigned to the CoCN bending mode. The two bands at 162 and 143 cm^{-1} in the Raman spectrum are assigned to the BaNC bending mode. The bands corresponding to the C–Co–C bending mode appear at 107, 93 and 62 cm^{-1} in the Raman spectrum.

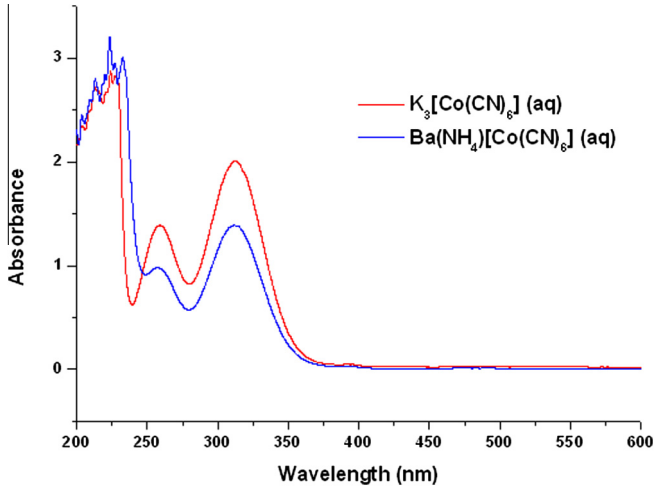

Fig. 3. UV–Vis absorption spectra between 200 and 600 nm of $Ba(NH_4)[Co(CN)_6]\cdot 4H_2O$ in aqueous solution and comparison with $K_3[Co(CN)_6]$ (aq).

3.3.3. Ammonium bands

The band at 3128 and 3122 cm^{-1} in the RT and LT IR spectra, respectively, are assigned to the anti-symmetric HNH stretching mode corresponding to the NH_4^+ ion. The bands at 3022 cm^{-1} in the IR spectra (3030 cm^{-1} in Raman) is assigned to the symmetric HNH stretching mode. The bands at 1414, 1400, 1384 and 1360 cm^{-1} in the room temperature IR spectrum are assigned to bending modes of the ammonium ion. The assignments were performed according to Nakamoto [32] and to spectroscopic data reported for related, ammonium-containing, molecules [33–34].

3.3.4. Water bands

In what follows, mode frequencies correspond to the LT IR spectrum unless otherwise stated. All fundamental water bands are expected in the IR region between 4000 and 200 cm^{-1}.

The presence of two kinds of crystallographically inequivalent water molecules in the lattice is evidenced by their IR characteristic vibration modes. The two narrow bands observed at 3626 and 3565 cm^{-1} could be assigned to O-H stretching modes corresponding to uncoordinated water molecules. The broad bands at 3453 and 3433 cm^{-1} are assigned to the O–H stretching modes corresponding to water molecules coordinated to Ba atoms as disclosed

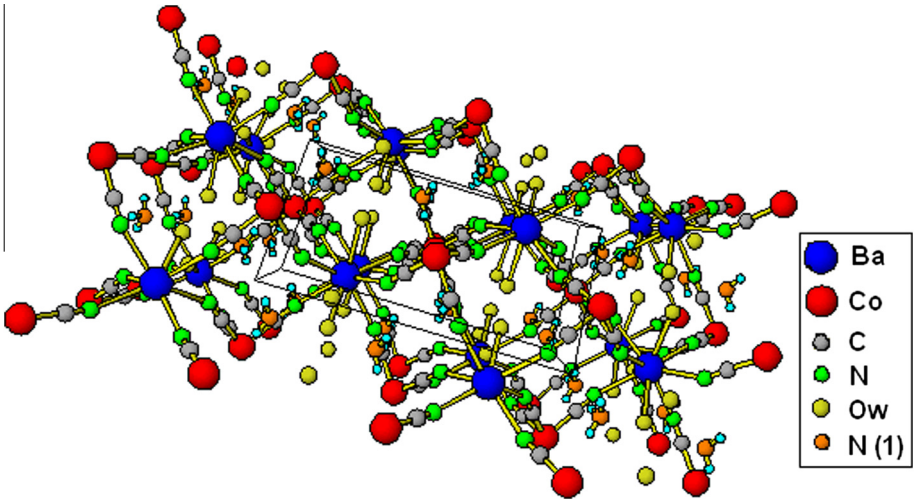

Fig. 2. Three-dimensional coordination network of $Ba(NH_4)[Co(CN)_6\cdot 4H_2O$ bridged by cyano groups. Uncoordinated water molecules are omitted for clarity.

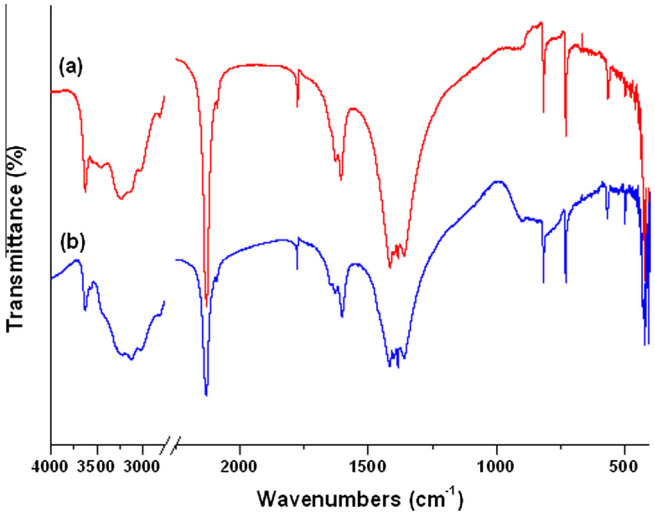

Fig. 4. FTIR spectra of $Ba(NH_4)[Co(CN)_6]\cdot 4H_2O$ at (a) −100 °C and (b) at room temperature.

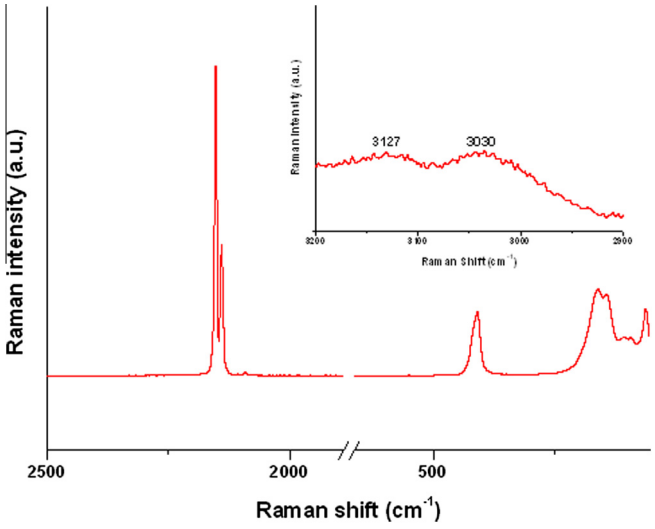

Fig. 5. Raman spectrum of $Ba(NH_4)[Co(CN)_6]\cdot 4H_2O$ at room temperature. The inset shows the expanded NH_4^+ stretching mode region between 3200 and 2900 cm^{-1}.

from the crystal structure. There are additional bands in this region (at 3273 and 3231 cm^{-1}) which can be assigned to the first overtone of the water deformations.

In the bending region two bands and a shoulder are observed at room temperature. This last feature increases its relative intensity significantly with the decrease of temperature. The band located at 1628 cm^{-1} is assigned to the bending mode of water molecules with a strong interaction with the Ba atom (coordinated water) and the band with lower intensity located at 1602 cm^{-1} is assigned to the bending mode of a weakly bonded water (uncoordinated or hydrogen bonded water). The weak band observed at 1646 cm^{-1} seems to confirm the interaction suggested by the spectral behavior in the ν OH region.

The libration modes of coordinated water appear in the spectral region between 820 and 300 cm^{-1} and generally are difficult to identify because they show low intensity and are overlapped with modes due to the hexacyanometallate anion. The increase of intensity and spectral shift upon cooling are very helpful to identify the libration bands. Due to the existence of the two unequivalent water molecules and in case they are asymmetric; six bands are expected in this region due to the following modes: wagging, rocking and twisting. This latter mode is inactive in symmetric water molecules but becomes active in asymmetric ones. The band at 817 cm^{-1} could be assigned to the rocking mode and the band at 730 cm^{-1} is assigned to the wagging mode. The frequency corresponding to the twisting mode of coordinated water molecules appears in the IR spectrum as a medium intensity band observed at 498 cm^{-1}.

3.4. Thermogravimetric (TG) and differential thermal (DT) analysis

The thermal behavior of the $Ba(NH_4)[Co(CN)_6]\cdot 4H_2O$ complex was studied by means TG and DT analysis. Fig. 6 shows TG and DT curves from the thermal decomposition of the complex measured in flowing air. The first step ends at 125 °C with a mass loss of 8.65% and it corresponds to the loss of two water molecules (theoretical value, 8.14%). The second step ends at 213 °C with a mass loss of 4.05% and it is attributed to the loss of one water molecule (theoretical value, 4.06%). These two steps are accompanied by two endothermic peaks observed at 110 and 192 °C in the DT curve. The third decomposition step occurs in the 215–355 °C temperature range and it can be attributed to the elimination of the remaining water molecule and the ammonium ion. It seems that the ammonium decomposition and the evolution of the last water molecule take place simultaneously. The next decomposition step occurs in the 360–460 °C range and it can be attributed to the elimination and oxidation of all the cyano groups, but part of the CO_2 formed in this combustion clearly gets adsorbed in the surface of the particles as carbonate species. The exothermic peak at 376 °C in the DT curve is attributed to the decomposition step mentioned previously. The mass loss observed at temperatures higher than 460 °C was assumed to be due to the decomposition of carbonate species adsorbed in the surface of the particles and $BaCO_3$ derived from the oxidation of the CN groups. The total mass loss observed at 1000 °C was 45.98% and it was in agreement with the theoretical value (44.78%) calculated for the formation of $BaCoO_3$ from the $Ba(NH_4)[Co(CN)_6]\cdot 4H_2O$ complex.

3.5. Characterization of products obtained by thermal decomposition of $Ba(NH_4)[Co(CN)_6]\cdot 4H_2O$ at different temperatures

In order to know what is the lower temperature of synthesis of $BaCoO_{3-\delta}$ perovskite-type oxide as a pure phase, thermal treatments of $Ba(NH_4)[Co(CN)_6]\cdot 4H_2O$ in air at different temperatures were carried out. The qualitative composition of the residues at different temperatures was determined using X'Pert Highscore program (version 3.0b). The PXRD patterns of the residues obtained by decomposition of $Ba(NH_4)[Co(CN)_6]\cdot 4H_2O$ heated at different temperatures during 6 h in air are shown in Fig. 7. When the complex was heated at 600 °C, the peaks attributed to $BaCO_3$ and Co_3O_4 were observed. When we increased the calcination temperature to 650 °C, some small peaks attributed to hexagonal $BaCoO_3$ were observed accompanied by some peaks assigned to $BaCO_3$ and Co_3O_4. When the complex was treated at 675 °C, all the peaks are attributable to hexagonal $BaCoO_3$. To the best of our knowledge this is the lower temperature at which $BaCoO_3$ was synthesized. This result demonstrated that the decomposition of cyano-complexes is the best way to prepare perovskite-type oxides at temperatures lower than in ceramic methods or other methods [17–21,35,36]. When the complex was treated at 700 °C no change was observed in the PXRD pattern with respect to the sample treated at 675 °C but in the treatment at 750 °C we observed a splitting of the peak at $2\theta = 31.9°$ and a widening of all peaks, as can be appreciated in Fig. 7.

The crystallographic structure of $BaCoO_3$ obtained at 675 °C has been refined by the Rietveld method. The pattern was fitted to the

Table 3
FTIR and Raman band frequencies with tentative vibration mode assignment for $Ba(NH_4)[Co(CN)_6]\cdot 4H_2O$.

IR solid (RT)[a]	IR solid (−100 °C)	Raman solid[b]	Approximate description of mode[c]
3625 w	3626 w	–	ν_a HOH uncoordinated water
3562 w	3565 w	–	ν_a HOH coordinated water
3541 br	3453 br	–	ν_s HOH uncoordinated water
3461 br	3433 br	–	ν_s HOH coordinated water
3288 w	3273 sh	–	2 ν_2 coordinated water
3243 sh	3231 sh	–	2 ν_2 uncoordinated water
3128 vw	3122 w	3127 (1)	ν_a NH_4^+
3022 w	3018 w	3030 (1)	ν_s NH_4^+
–	–	2153 (100)	ν_s CN
–	–	2141 (42)	ν_s CN
2131 s	2132 s	–	ν_a CN
2090 w	3091 w	2091 (1)	ν $^{13}C^{14}N$
1644 sh	1646 w	–	δ H_2O [d]
1627 w	1628 w	–	δ H_2O coordinated
1606 m	1602 m	–	δ H_2O uncoordinated
1414 m	1415 m	–	δ NH_4^+
1400 m	1400 m	–	
1384 m	1384 m	–	
1360 m	1360 m	–	
817 vw	817 w	–	ρ H_2O
729 vw	730 w	–	ω H_2O
565 w	568 w	–	ν Co–C
498 w	498 m	–	$\tau\omega$ H_2O
419 m	421 m	417 sh	δ CoCN
–	–	409 (20)	ν Co–C
–	–	162 (27)	δ BaNC
–	–	143 (26)	δ BaNC
–	–	107 (12)	δ C–Co–C
–	–	93 (12)	δ C–Co–C
–	–	62 (21)	δ C–Co–C

[a] sh, shoulder; br, broad; vs very strong; s, strong; m, medium; w, weak; vw, very weak.
[b] Relative bands heights in parentheses.
[c] The symbols ν, δ, ρ, ω represent stretching, deformation, rocking and wagging modes; ν_2 corresponds to the H_2O bending mode.
[d] See text.

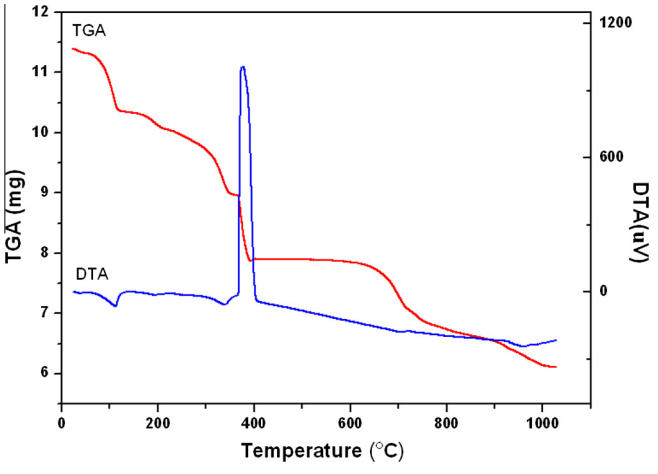

Fig. 6. TGA and DTA curves for $Ba(NH_4)[Co(CN)_6]\cdot 4H_2O$ at 5°/min in air flow.

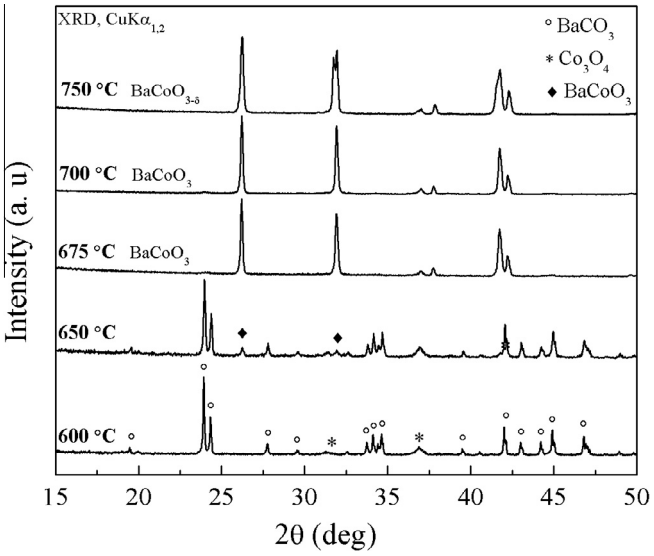

Fig. 7. PXRD patterns of the residues obtained by decomposition of $Ba(NH_4)[Co(CN)_6]\cdot 4H_2O$.

hexagonal space group $P6_3/m\ m\ c$ (No. 194), with unit-cell parameters $a = b = 5.6102(2)$ Å and $c = 4.7668(2)$ Å. This structure presents a 2H-type perovskite structure, consisting of infinite chains of CoO_6 face-sharing octahedra, running along the c-direction. The Rietveld refinement from the PXRD data is displayed in Fig. 8. The two minor impurities Co_3O_4 (space group *Fd-3m*) and $BaCO_3$ (space group *Pmcn*) were included in the refinement as second and third crystallographic phases. From the refined scale factors, there were estimated 0.8% and 1.04% of impurities contents, respectively. Results of the refined structural parameters and relevant inter-atomic distances and angles for $BaCoO_3$ prepared at 675 °C are shown in Table 4.

Fig. 9 display a view of the crystal structure of $BaCoO_3$, showing that it contains chains of CoO_6 octahedra sharing faces along the c axis (a) and a projection of the crystal structure onto the *ab* plane (b). As can be seen in Table 4, Ba–O distances in the BaO_{12} polyhedron have an average <Ba–O> bond length of 2.87 Å which compares well with the value expected from the sum of the ionic radii of 3.01 Å for Ba^{2+} (for 12 coordination) = 1.75 Å and O^{2-} (6 coordinated) = 1.26 Å [37]. A distance of 2.38 Å for Co–Co distances

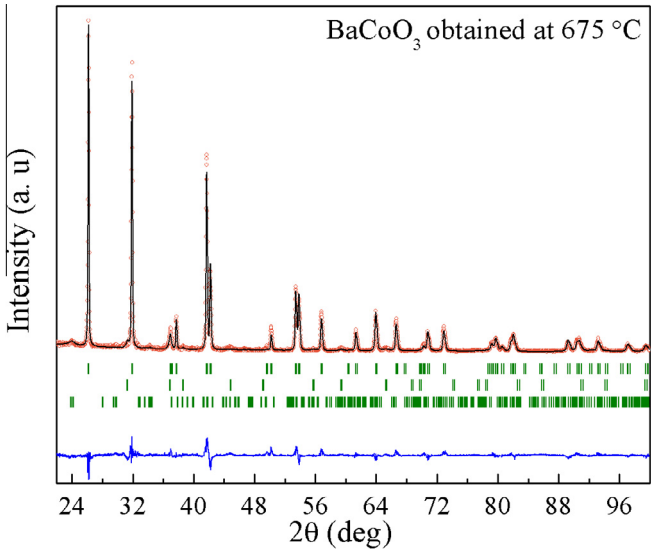

Fig. 8. Refined PXRD pattern for $BaCoO_3$ obtained at 675 °C. Observed (circles), calculate (solid line) and difference (solid line at the bottom). The vertical lines correspond to the positions of Bragg reflections (1 = $BaCoO_3$, 2 = Co_3O_4 (0.8%) and 3 = $BaCO_3$ (1.04%)).

Table 4
Structural parameters, main inter-atomic distances (Å) and selected angles (°) for the $BaCoO_3$ phase obtained at 675 °C after Rietveld refinement of PXRD at room temperature in the hexagonal space group $P6_3/m$ m c; cell parameters: $a = b = 5.6102(2)$ Å, $c = 4.7668(2)$ Å and $V = 129.9(1)$ Å^3. $R_{Bragg} = 5.74\%$ and $\chi^2 = 2.94$.

Atom	Wyckoff site	x	y	z
Ba	2d	1/3	2/3	3/4
Co	2a	0	0	0
O	6h	0.1564(1)	−0.1564(1)	1/4
Distances (Å) and angles (deg)				
Ba–O (x6)	2.9387(3)	Co–O (x6)	1.9311(3)	
Ba–O (x6)	2.8072(5)	Co–Co (x2)	2.3834(1)	
<Ba–O>	2.8730	Co–O–Co	76.21(2)	

are indicative of face-sharing CoO_6 octahedra. For the Co–O bonds the average length of 1.93 Å is in good agreement with the sum of ionic radii of six-coordinated Co^{4+} (HS) ions (0.67 Å) and O^{2-} (1.26 Å) [37].

The sample prepared at 700 °C showed the same X-ray diffraction pattern. Refined parameters are very similar to the one of the sample prepared at 675 °C (not shown), however the diffractogram for the sample prepared at 750 °C showed a clear splitting of reflections at $2\theta = 31.9°$ and a widening of several others, which could not be refined with the hexagonal model. We attempted to refine this diffractogram with a C-centered orthorhombic one by using the unit cell transformation:

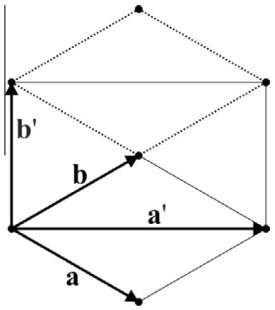

where: $a_{orth} = a_{hex}$, $b_{orth} = b_{hex}\sqrt{3}$, $c_{orth} = c_{hex}$. Using the hexagonal parameters informed in Table 4, we obtained the equivalent orthorhombic cell parameters $a_{orth} = 5.6102(2)$ Å; $b_{orth} = 9.7171(2)$ Å and $c_{orth} = 4.7668(2)$ Å. We use these orthorhombic cell parameters as the starting values for a Full Profile Refinement (Le Baíls method). The C centered space group that takes into account the observed systematic absences was *Cmcm*. The final refined parameters of the orthorhombic phase are: $a = 5.6099(2)$ Å $b = 9.7865(2)$ Å and $c = 4.7576(2)$ Å. This new orthorhombic phase obtained by this method was not informed previously probably because by using other conventional synthetic methods it is not possible to explore this temperature range. It is expected that this new orthorhombic phase is a small distortion of the hexagonal one produced by a very small amount of oxygen vacancies. More studies are in progress to determine the structural model of this new phase.

4. Conclusions

The complex $Ba(NH_4)[Co(CN)_6]\cdot 4H_2O$ was synthesized for the first time and its crystal structure determined by single-crystal X-ray diffraction methods. The complex crystallizes in the hexagonal $P6_3/m$ space group with $a = b = 7.6882(2)$ Å, $c = 14.4764(4)$ Å, and $Z = 2$ molecules per unit cell. In this structure the Ba^{2+} ions are nine-coordinated to six nitrogen atoms from CN groups and three oxygen atoms from crystal water in the form of BaN_6O_3

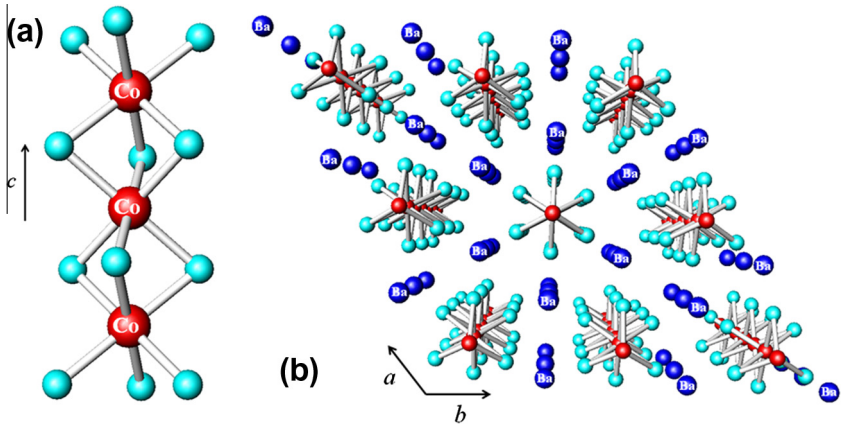

Fig. 9. Two different views of the crystal structure of $BaCoO_3$. (a) Individual chain of CoO_6 octahedra sharing faces along the c axis. (b) Projection of the crystal structure onto the crystal *ab* plane.

group. On the other hand, six carbon atoms are coordinated to a cobalt atom in octahedral geometry. One non-coordinated water molecule was observed in the structure.

The Infrared and Raman spectra were measured and the observed bands assigned to normal modes of the cobalticyanide anion, the ammonium ion, and the water molecules. The UV–Vis spectrum of the complex in aqueous solution shows two absorption bands at 259 and 313 nm corresponding to $^1T_{2g} \leftarrow {}^1A_{1g}$ and $^1T_{1g} \leftarrow {}^1A_{1g}$ transitions, respectively.

The thermal decomposition of $Ba(NH_4)[Co(CN)_6]\cdot 4H_2O$ in air was studied using TGA/DTA analysis. The first and the second steps in the thermal decomposition of the complex correspond to the elimination of three water molecules. The third step is attributed to the elimination of the remaining water molecule together with the elimination of the ammonium ion. The next step is attributed to the elimination and oxidation of CN groups. The last step corresponds to the thermal decomposition of carbonate species adsorbed in the surface and $BaCO_3$ to form the mixed oxide $BaCoO_3$ as final product.

The thermal treatments of $Ba(NH_4)[Co(CN)_6]\cdot 4H_2O$ in air produced the mixed oxide $BaCoO_3$ at 675 °C, a very low temperature of synthesis compared with ceramic methods. It indicates that the thermal decomposition of the cyano-complexes is the best way to prepare perovskite-type oxides. At 750 °C a new orthorhombic poly-type is obtained mixed with the hexagonal one which is apparently associated with the presence of oxygen vacancies.

Acknowledgements

D.M.G. and A.B.A. thank CIUNT (Project 26D-411) and CONICET (PIP 0629) for financial support. R.E.C. thanks support from CONICET (PIP #11220090100995) and SECyT-UNC (Project 162/12). D.M.G. and F.P. thank CONICET for fellowships.

O.E.P. thanks CONICET (PIP 1529), and ANPCyT (PME06 2804 and PICT06 2315).

Appendix A. Supplementary data

CCDC 978121 contains the supplementary crystallographic data for $Ba(NH_4)[Co(CN)_6]\cdot 4H_2O$. These data can be obtained free of charge via http://www.ccdc.cam.ac.uk/conts/retrieving.html, or from the Cambridge Crystallographic Data Centre, 12 Union Road, Cambridge CB2 1EZ, UK; fax: (+44) 1223-336-033; or e-mail: deposit@ccdc.cam.ac.uk. Supplementary data associated with this article can be found, in the online version, at http://dx.doi.org/10.1016/j.poly.2014.02.014.

References

[1] S. Ferlay, T. Mallah, R. Ouahes, P. Veillet, M. Verdaguer, Nature 378 (1995) 701.
[2] R. Martinez-García, M. Knobel, G. Goya, M.C. Gimenez, F.M. Romero, E. Reguera, J. Phys. Chem. Solids 67 (2006) 2289.
[3] J. Rodriguez-Hernánez, A. Gómez, E. Reguera, J. Phys. D Appl. Phys. 40 (2007) 6076.
[4] R. Martinez-García, L. Reguera, M. Knobel, E. Reguera, J. Phys.: Condens. Matter 19 (2007) 056202.
[5] A. Kumar, S.M. Yusuf, L. Keller, J.V. Yakhmi, J.K. Srivastava, P.L. Paulose, Phys. Rev. B 75 (2007) 224419.
[6] H. Yasuda, Y. Fujiwara, N. Mizuno, M. Misono, J. Chem. Soc., Faraday Trans. 90 (1994) 1183.
[7] B.P. Barbero, J.A. Gamboa, L.E. Cadús, Appl. Catal. B 65 (2006) 21.
[8] Y. Teraoka, K. Nakano, W. Shangguan, S. Kagawa, Catal. Today 27 (1996) 107.
[9] R.J. Bell, G.J. Millar, J. Drennan, Solid State Ionics 131 (2000) 211.
[10] P.V. Gosavi, R.B. Biniwale, Mater. Chem. Phys. 119 (2010) 324.
[11] H.M. Zhang, Y. Teraoka, N. Yamazoe, Chem. Lett. 16 (1987) 665.
[12] S. Royer, F. Bérubé, S. Kaliaguine, Appl. Catal. A 282 (2005) 273.
[13] W. Li, M.W. Zhou, J.I. Shi, Matter. Lett. 58 (2004) 365.
[14] M. Yuasa, K. Shimanoe, Y. Teraoka, N. Yamazoe, Catal. Today 126 (2007) 313.
[15] K. Tsuchida, S. Takase, Y. Shimizu, Sens. Matter. 16 (2004) 171.
[16] M. Popa, J. Frantti, M. Kakihana, Solid State Ionics 154 (2002) 437.
[17] P.K. Gallagher, Mater. Res. Bull. 3 (1968) 225.
[18] D.M. Gil, M.C. Navarro, M.C. Lagarrigue, J. Guimpel, R.E. Carbonio, M.I. Gómez, J. Therm. Anal. Calorim. 103 (3) (2011) 889.
[19] D.M. Gil, M. Avila, E. Reguera, S. Pagola, M.I. Gómez, R.E. Carbonio, Polyhedron 33 (2012) 450.
[20] D.M. Gil, R.E. Carbonio, M.I. Gómez, J. Mol. Struct. 1041 (2013) 23.
[21] D.M. Gil, G. Nieva, D.G. Franco, M.I. Gómez, R.E. Carbonio, Mater. Chem. Phys. 141 (2013) 355.
[22] CrysAlisPro, Oxford Diffraction Ltd., version 1.171.33.48 (release 15–09-2009 CrysAlis171.NET).
[23] G.M. Sheldrick, SHELXS-97, Program for Crystal Structure Resolution, Univ. of Göttingen, Göttingen, Germany, 1997.
[24] G.M. Sheldrick, SHELXL-97, Program for Crystal Structure Analysis, Univ. of Göttingen, Göttingen, Germany, 1997.
[25] (a) MISSYM (ADDSYM) Algorith Y. LePage, J. Appl. Crystallogr. 20 (1987) 264; (b) A.L. Spek, J. Appl. Crystallogr. 21 (1988) 578.
[26] R.A. Young, The Rietveld method, Oxford Scientifics Publications, UK, 1995.
[27] J. Rodriguez-Carbajal, Physica B 192 (1993) 55.
[28] C.K. Johnson, ORTEP-II. A Fortran Thermal-Ellipsoid Plot Program. Report ORNL-5318, Oak Ridge National Laboratory, Tennessee, USA, 1976.
[29] A.R. Riordan, A. Jansma, S. Fleischman, D.B. Green, D.R. Mulford, Chem. Educator 10 (2005) 115.
[30] J. Rodriguez-Hernández, E. Reguera, E. Lima, J. Balmaseda, R. Martinez-García, H. Yee-Madeira, J. Phys. Chem. Solids 68 (2007) 1630.
[31] Y. Yukawa, S. Iggarashi, T. Kawaura, H. Miyamoto, Inorg. Chem. 35 (1996) 7399.
[32] K. Nakamoto, Infrared and Raman Spectra of Inorganic and Coordination Compounds, fifth ed., Wiley-Interscience, New York, 1997.
[33] H.A. De Abreu, A.L.S. Junior, A.A. Leitão, L.R.V. De Sá, M.C.C. Ribeiro, R. Diniz, L.F.C. De Oliveira, J. Phys. Chem. A 113 (2009) 6446.
[34] M. Mookherjee, S.A.T. Redfern, M. Zhang, D.E. Harlov, Eur. J. Mineral. 14 (2002) 1033.
[35] C. de la Calle, J.A. Alonso, M.T. Fernández-Díaz, Z. Naturforsch. 63b (2008) 647.
[36] S. Hébert, V. Pralong, D. Pelloquin, A. Maignan, J. Magn. Magn. Mater. 316 (2007) 394.
[37] R.D. Shannnon, Acta Crystallogr., Sect. A 32 (1976) 751.